

Probing the nature of electroweak symmetry breaking with Higgs boson pairs in ATLAS

Bartłomiej Żabiński
On behalf of the ATLAS Collaboration
*The Henryk Niewodniczański
Institute of Nuclear Physics
Polish Academy of Sciences*

Constraints on the Higgs boson trilinear self-coupling modifier κ_λ and non-SM HHVV coupling strength κ_{2V} are set by combining di-Higgs boson analyses using $b\bar{b}b\bar{b}$, $b\bar{b}\tau^+\tau^-$, $b\bar{b}\gamma\gamma$, $b\bar{b}ll + E_T^{\text{miss}}$ and multileptons decay channels. The data used in these analyses were recorded by the ATLAS detector at the Large Hadron Collider in proton–proton collisions at $\sqrt{s} = 13$ TeV and correspond to an integrated luminosity of 126–140 fb^{-1} . The combination of the di-Higgs analyses sets an upper limit of signal strength $\mu_{HH} < 2.9$ at 95% confidence level on the di-Higgs production and constraints for κ_λ between -1.2 and 7.2. The obtained confidence interval for κ_{2V} coupling modifier is [0.6,1.5]. The Higgs effective field theory has been tested, and constraints on two Wilson coefficients have been added.

1 Introduction

The discovery of the Higgs boson by ATLAS¹ and CMS² experiments at the CERN Large Hadron Collider (LHC)³ opened opportunities to measure the boson’s properties and test new hypotheses. In the Standard Model (SM)^{4,5,6} Higgs boson potential^{7,8} provides spontaneous electroweak symmetry breaking that gives rise to its self-interactions. The Higgs boson self-interactions can be described among others by trilinear self-coupling λ_{HHH} that can be predicted at lowest order from Fermi constant G_F ⁹ and the Higgs mass m_H expressed by equation (1):

$$\lambda_{HHH} = \frac{m_H^2 G_F}{\sqrt{2}} \quad (1)$$

The validity of the SM in the Higgs sector can be tested using the ‘kappa framework’^{10,11}, in which a coupling modifier κ_m is defined as the ratio of the coupling strength between the particle m and Higgs boson to its SM value. The deviation of κ_m from unity would indicate physics processes beyond SM. For di-Higgs production κ_λ , κ_t , κ_V and κ_{2V} are considered. The κ_λ is Higgs boson self-coupling modifier. The κ_V and κ_t describe modifying the SM Higgs boson coupling to W or Z bosons and up-type quarks, respectively. The κ_{2V} is related to the VVHH interaction vertex. The κ_λ coupling modifiers can be measured in the gluon-gluon fusion process (ggF HH) and vector boson fusion (VBF). The κ_V and κ_{2V} can be measured in the VBF processes. At the LHC, Higgs boson pair-production is dominated by ggF processes and the overall predicted cross-section in the SM is $\sigma_{\text{ggF}}^{\text{SM}}(pp \rightarrow HH) = 31.1_{-7.1}^{+1.9}(\text{scale} + m_{\text{top}}) \pm 09(\text{PDF} + \alpha_s)$ fb at $\sqrt{s} = 13$ TeV^{12,13,14,15,16}. The second largest Higgs pair-production process at the LHC is VBF with $\sigma_{\text{VBF}}^{\text{SM}} = 1.73 \pm 0.04$ fb at $\sqrt{s} = 13$ TeV^{17,18,19}. The deviation of the double Higgs boson production from the SM can also be tested using Higgs Effective Field Theory (HEFT)^{20,21}. The HEFT is a framework used to describe the dynamics of the Higgs boson without the assumption of the SM’s linear realization of electroweak

symmetry breaking. The HEFT Lagrangian describes ggF double Higgs boson production at leading order (LO) by five relevant operators and their associated Wilson coefficients c_{tth} , c_{ggh} , c_{hhh} , c_{gghh} , and c_{tthh} . The HEFT allows for a more flexible, non-linear interpretation of Higgs interactions. This approach can accommodate scenarios where the Higgs sector exhibits complex or exotic behavior, such as strong dynamics or deviations from SM predictions. HEFT is particularly useful for exploring anomalous Higgs couplings and interactions in experimental data, providing a broader theoretical foundation for understanding the Higgs boson's role in particle physics. Figure 1 represents LO diagrams of the ggF and VBF production processes at the LHC featuring coupling modifiers described above.

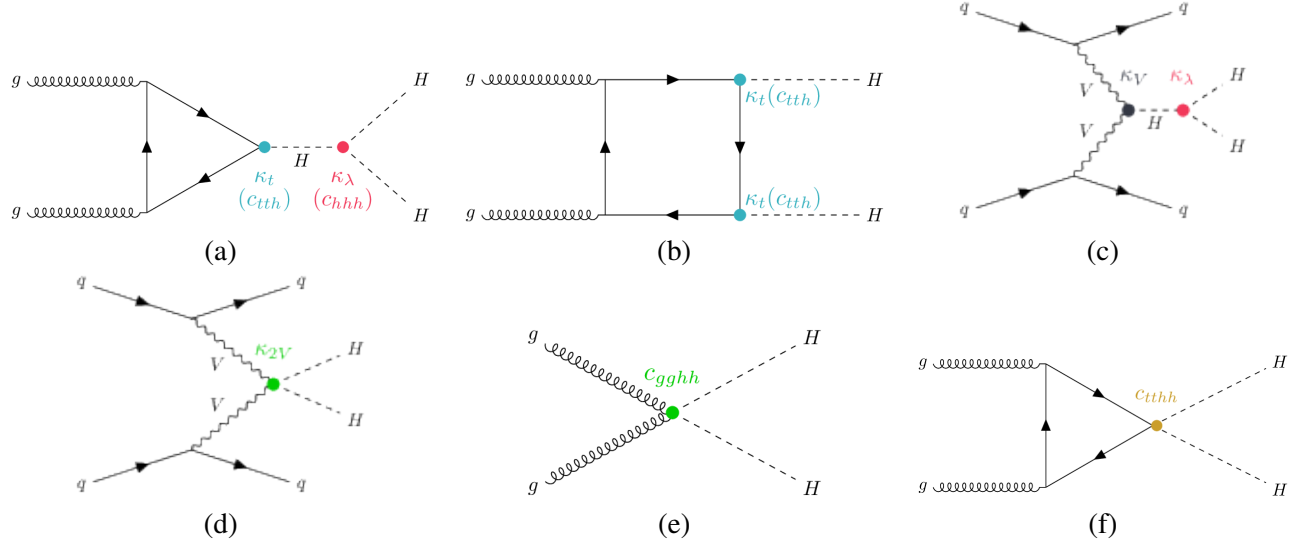


Figure 1 – Examples of LO Feynman diagrams for Higgs boson pair production, via ggF production (a), (b), (e), (f), and via VBF production (c), and (d). Diagrams (e) and (f) manifest only when deviations from the SM predictions are present in the HEFT Wilson coefficients c_{gghh} and c_{tthh} .²⁷

2 Higgs boson pair production in ATLAS

The Higgs pair-production is measured in different decay channels $b\bar{b}b\bar{b}$ ²², $b\bar{b}\gamma\gamma$ ²³, $b\bar{b}\tau\tau$ ²⁴, $b\bar{b}ll$ ²⁵ and with leptons in the final state²⁶. The combination of mentioned channels²⁷ will be discussed in this report. Analysis-specific details can be found in the above-referenced publications. The first measured parameter of the combined results is signal strength μ_{HH} defined as a ratio of di-Higgs production cross-section including only ggF and VBF processes to its SM prediction of $32.8^{+2.1}_{-7.2}$ fb. The expected and observed upper limits on μ_{HH} at 95% CL are 2.4 and 2.9, respectively. The best-fit value obtained from the fit to the data $\mu_{HH}=0.5^{+1.2}_{-1.0}$ is compatible with the SM prediction of unity, with a p -value of 0.64. The obtained limits of μ_{HH} for each particular channel entering the combination and the results of the combination itself are shown in Figure 2.

The combination constraints for κ_λ and κ_{2V} coupling modifiers are shown in Figure 3. Presented limits for κ_λ and κ_{2V} are obtained by using the values of the test statistic ($-2\ln\Lambda$) as a function of κ_λ in the asymptotic approximation and including the theoretical uncertainty of the cross-section predictions. The obtained limits for κ_λ for each discussed analysis are collected in Table 1, and the combination constraint at 95% CL is $-1.2 < \kappa_\lambda < 7.2$ (observed) and $-1.6 < \kappa_\lambda < 7.2$ (expected). The κ_{2V} coupling modifier for each mentioned channel and their combination have been obtained by fixing all other coupling modifiers to unity and with the expected value derived from the SM hypothesis. The expected and observed at 95% CL combined constraint for κ_{2V} are $0.4 < \kappa_{2V} < 1.6$ and $0.6 < \kappa_{2V} < 1.5$, respectively. Table 1 includes κ_{2V} constraints for each channel under combination.

Figure 4 represents two Wilson's coefficients, obtained after combination of the three most sensitive decay channels $b\bar{b}b\bar{b}$, $b\bar{b}\gamma\gamma$, and $b\bar{b}\tau\tau$. The constraints for c_{gghh} and c_{tthh} with all other coefficients fixed to the SM predictions have been obtained. The observed interval at 95% CL on c_{gghh} is $-0.38 < c_{gghh} < 0.49$ which is compatible with the SM predictions with a p -value of 0.087. Similarly, the observed interval at

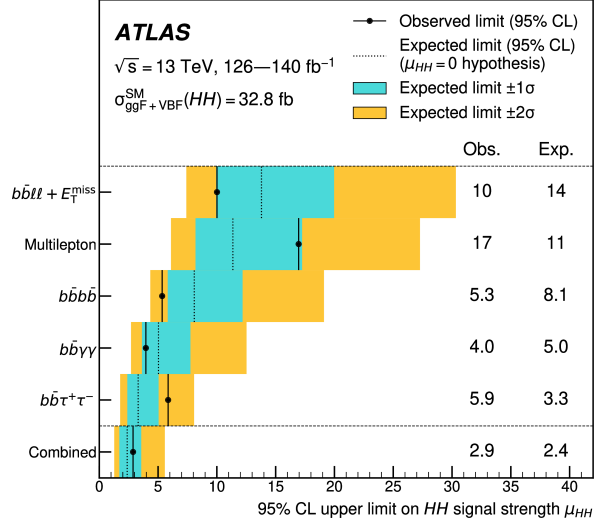


Figure 2 – Observed and expected 95% CL upper limits on the signal strength for di-Higgs production from the $b\bar{b}b\bar{b}$, $b\bar{b}\tau^+\tau^-$, $b\bar{b}\gamma\gamma$, $b\bar{b}l\bar{l} + E_T^{\text{miss}}$, multilepton decay channels, and their statistical combination. The value $m_H = 125$ GeV is assumed when deriving the predicted SM cross-section. The expected limit and the corresponding error bands are derived assuming the absence of the HH process and with all nuisance parameters profiled to the observed data.²⁷

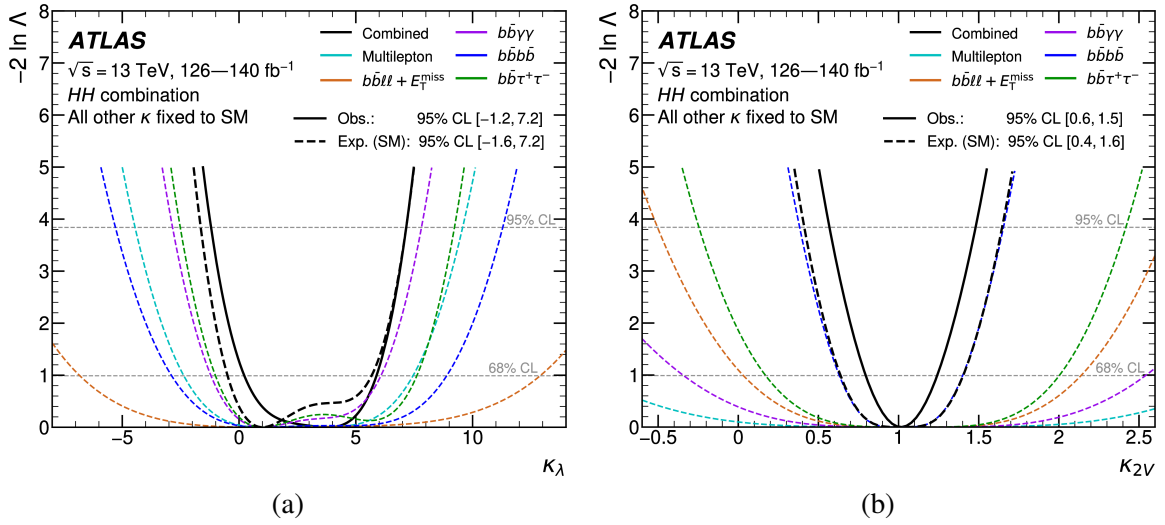


Figure 3 – The observed (solid lines) and expected (dashed lines) values of the test statistic ($-2 \ln \Lambda$) as a function of (a) κ_λ and (b) κ_{2V} . The different colors represent the results of the the individual channels. The combination results are represented by black color.²⁷

	$b\bar{b}b\bar{b}$	$b\bar{b}\tau\tau$	$b\bar{b}\gamma\gamma$	$b\bar{b}l\bar{l}$	ML
Observed 95% CL	$-3.5 < \kappa_\lambda < 11.3$	$-3.1 < \kappa_\lambda < 9.0$	$-1.4 < \kappa_\lambda < 6.9$	$-6.2 < \kappa_\lambda < 13.3$	$-6.2 < \kappa_\lambda < 11.6$
Expected 95% CL	$-5.4 < \kappa_\lambda < 11.4$	$-2.5 < \kappa_\lambda < 9.3$	$-2.8 < \kappa_\lambda < 7.8$	$-8.1 < \kappa_\lambda < 15.5$	$-4.5 < \kappa_\lambda < 9.6$
Observed 95% CL	$0.0 < \kappa_{2V} < 2.1$	$-0.5 < \kappa_{2V} < 2.7$	$-0.5 < \kappa_{2V} < 2.7$	$-0.17 < \kappa_{2V} < 2.4$	$-2.5 < \kappa_{2V} < 4.6$
Expected 95% CL	$-0.1 < \kappa_{2V} < 2.1$	$-0.2 < \kappa_{2V} < 2.4$	$-1.1 < \kappa_{2V} < 3.3$	$-0.51 < \kappa_{2V} < 2.7$	$-1.9 < \kappa_{2V} < 4.1$

Table 1: Summary of κ_λ and κ_{2V} observed and expected constraints for the $HH \rightarrow b\bar{b}b\bar{b}$, $HH \rightarrow b\bar{b}\tau\tau$, $HH \rightarrow b\bar{b}\gamma\gamma$, $HH \rightarrow b\bar{b}l\bar{l} + E_T^{\text{miss}}$ and multilepton (ML) analyses. Limits are obtained using the test statistic ($-2 \ln \Lambda$) in the asymptotic approximation. The expected constraints are derived under the SM assumption. All other coupling modifiers are fixed to the SM value.

95% CL on c_{tthh} is $-0.19 < c_{tthh} < 0.70$ and is compatible with the SM prediction with a p-value of 0.16.

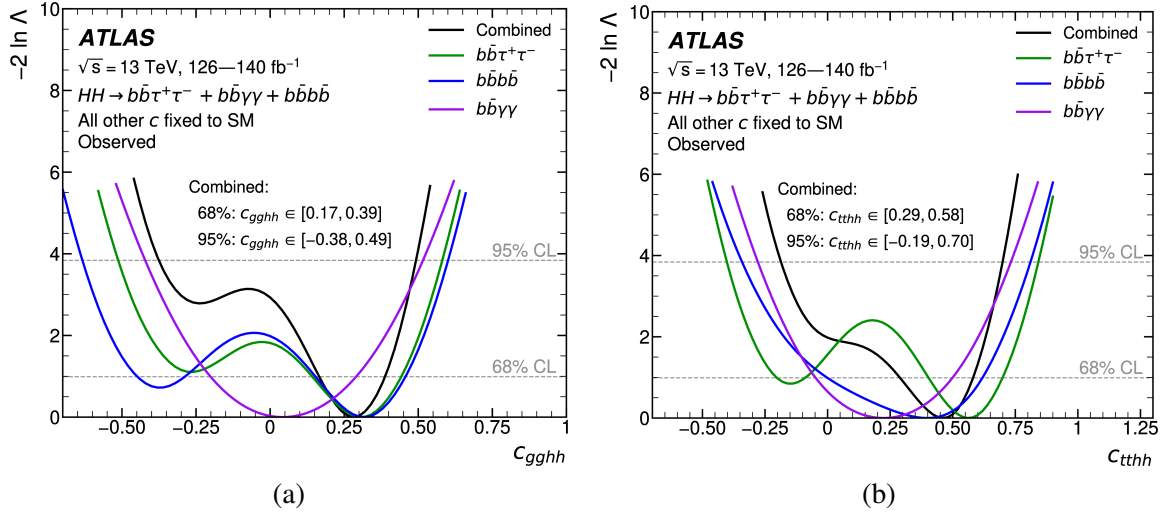


Figure 4 – The observed test statistic ($-2\ln\Lambda$) as a function of (a) c_{gghh} and (b) c_{tthh} . The different colors represent the results of the individual channels. The combination results are shown in black.²⁷

3 Conclusions

The double Higgs production searches offer a unique opportunity to investigate the mechanism of electroweak symmetry-breaking. The measurement of λ_{HHH} is challenging due to very small cross-sections of the di-Higgs production processes. Constraints are set on the signal strength μ as well as on κ_λ and κ_{2V} . The obtained limits intervals for each considered channel are wide, but by the combination of all channels, the constraints have been limited to $0.1 < \kappa_{2V} < 2.0$ and $-0.6 < \kappa_\lambda < 6.6$. The constraints of the two HEFT Wilson coefficients have been estimated as well. No deviations from the SM have been observed. The di-Higgs searches are also a good probe for beyond SM heavy resonance searches^{28,29,30,31}. However, the ATLAS experiment is in the Run-3 data-taking phase, where it is expected to collect two times more data than during Run-2 and finally reach LHC runs with high luminosity. That significant amount of data will offer an unprecedented opportunity to increase the sensitivity of the mentioned channels and provide better limits for the coupling modifiers.

Funding informaion This work is supported in part by the Polish Ministry of Education and Science project no.2022/WK/08, and Polish National Science Center OPUS no. 2022/47/B/ST2/03059.

References

1. ATLAS Collaboration, *Observation of a new particle in the search for the Standard Model Higgs boson with the ATLAS detector at the LHC*, Physics Letters B **716** (2012) 1, arXiv:1207.7214 [hep-ex].
2. CMS Collaboration, *Observation of a new boson at a mass of 125 GeV with the CMS experiment at the LHC*, Physics Letters B **716** (2012) 30, arXiv:1207.7235.
3. L. Evans, P. Bryant (Eds.), *LHC Machine*, JINST **3** (2008) S08001.
4. S.L. Glashow, *Partial-symmetries of weak interactions*, Nucl. Phys. **22** (1961) 579.
5. A.Salam, *Weak and Electromagnetic Interactions*, Conf. Proc. C **680519** (1968). Proceedings of the eight Nobel symposium.
6. S.Weinberg, *A model of leptons*, Phys. Rev. Lett. **19** (1967) 1264.
7. F.Englert and R.Brout, *Broken Symmetry and the Mass of Gauge Vector Mesons*, Phys. Rev. Lett **13** (1964) 321.
8. P.W.Higgs, *Broken symmetries, massless particles and gauge fields*, Phys. Rev. Lett. **12** (1964) 132.

9. Particle Data Group, R.L. Workman et al. *Review of Particle Physics*, PTEP **2022** (2022) 083C01.
10. LHC Higgs Cross Section Working Group, S. Heinemeyer et al., *Handbook of LHC Higgs Cross Sections:3. Higgs Properties*, CERN-2013-004 (CERN, Geneva, 2013), arXiv:1307.1347 [hep-ph].
11. LHC Higgs Cross Section Working Group, D. de Florian et al., *Handbook of LHC Higgs Cross Sections:4. Description of Nature of the Higgs Sector*, CERN-2017-002-M (CERN, Geneva, 2017), arXiv:1610.07922 [hep-ph].
12. S. Dawson, S. Dittmaier and M. Spira, *Neutral Higgs-boson pair production at hadron colliders: QCD corrections*, Phys. Rev. D **58** (1998) 115012, arXiv: hep-ph/9805244 [hep-ph].
13. J. Baglio et al., *gg→HH: Combined uncertainties*, Phys. Rev. D **103** (2021) 056002, arXiv: 2008.11626 [hep-ph].
14. M. Grazzini et al., *Higgs boson pair production at NNLO with top quark mass effects*, JHEP **05** (2018) 059, arXiv: 1803.02463 [hep-ph].
15. G. Heinrich, S. P. Jones, M. Kerner, G. Luisoni and L. Scyboz, *Probing the trilinear Higgs boson coupling in di-Higgs production at NLO QCD including parton shower effects*, JHEP **06** (2019) 066, arXiv: 1903.08137 [hep-ph].
16. D. de Florian and J. Mazzitelli, *Higgs Boson Pair Production at Next-to-Next-to-Leading Order in QCD*, Phys. Rev. Lett. **111** (2013) 201801, arXiv: 1309.6594 [hep-ph].
17. R. Frederix, S. Frixione, V. Hirschi, F. Maltoni, O. Mattelaer, P. Torrielli, E. Vryonidou, and M. Zaro, *Higgs pair production at the LHC with NLO and parton-shower effects*, Phys. Lett. B **732** (2014) 142, arXiv:1401.7340.
18. Frédéric A. Dreyer, Alexander Karlberg, *Fully differential Vector-Boson Fusion Higgs Pair Production at Next-to-Next-to-Leading Order*, Phys. Rev. D **99**, 074028 (2019), arXiv:1811.07918 [hep-ph].
19. F. A. Dreyer, A. Karlberg, J.-N. Lang and M. Pellen, *Precise predictions for double-Higgs production via vector-boson fusion*, Eur. Phys. J. C **80** (2020) 1037, arXiv: 2005.13341 [hep-ph].
20. R. Alonso and M.B. Gavela and L. Merlo and S. Rigolin and J. Yepes, *The effective chiral Lagrangian for a light dynamical “Higgs particle”*, Phys. Lett. B **722**, 330 (2013), arXiv:1212.3305 [hep-ph].
21. Gerhard Buchalla, Oscar Catà, Claudius Krause, *Complete electroweak chiral Lagrangian with a light Higgs at NLO*, Nuc. Phys. B **880**, 552 (2014), arXiv:1307.5017 [hep-ph].
22. ATLAS Collaboration, *Search for nonresonant pair production of Higgs bosons in the $b\bar{b}b\bar{b}$ final state in pp collisions at $\sqrt{s} = 13$ TeV with the ATLAS detector*, Phys. Rev. D **108** (2023) 052003, arXiv:2301.03212 [hep-ex].
23. ATLAS Collaboration, *Studies of new Higgs boson interactions through nonresonant HH production in the $b\bar{b}\gamma\gamma$ final state in pp collisions at $\sqrt{s} = 13$ TeV with the ATLAS detector*, JHEP **01** (2024) 066, arXiv:2310.12301 [hep-ex].
24. ATLAS Collaboration, *Search for the nonresonant production of Higgs boson pairs via gluon fusion and vector-boson fusion in the $b\bar{b}\tau^+\tau^-$ final state in proton-proton collisions at $\sqrt{s} = 13$ TeV with the ATLAS detector*, Phys. Rev. D **110** (2024) 032012, arXiv:2404.12660 [hep-ex].
25. ATLAS Collaboration, *Search for non-resonant Higgs boson pair production in the $2b + 2l + E_T^{miss}$ final state in pp collisions at $\sqrt{s} = 13$ TeV with the ATLAS detector*, JHEP **02** (2024) 037, arXiv:2310.11286 [hep-ex].
26. ATLAS Collaboration, *Search for non-resonant Higgs boson pair production in final states with leptons, taus, and photons in pp collisions at $\sqrt{s} = 13$ TeV with the ATLAS detector*, JHEP **08** (2024) 164, arXiv:2405.20040 [hep-ex].
27. ATLAS Collaboration, *Combination of Searches for Higgs Boson Pair Production in pp Collisions at $\sqrt{s} = 13$ TeV with the ATLAS Detector*, Phys. Rev. Lett. **133** (2024) 10181, arXiv:2406.09971 [hep-ex].
28. ATLAS Collaboration, *Search for Higgs boson pair production in the two bottom quarks plus two photons final state in pp collisions at $\sqrt{s} = 13$ TeV with the ATLAS detector*, Phys. Rev. D **106** (2022) 052001, arXiv:2112.11876 [hep-ex].
29. ATLAS Collaboration, *Search for resonant and non-resonant Higgs boson pair production in the $b\bar{b}\tau^+\tau^-$ decay channel using 13 TeV pp collision data from the ATLAS detector*, JHEP **07** (2023) 040, arXiv:2209.10910 [hep-ex].

30. ATLAS Collaboration, *Search for resonant pair production of Higgs bosons in the $b\bar{b}b\bar{b}$ final state using pp collisions at $\sqrt{s} = 13$ TeV with the ATLAS detector*, Phys. Rev. D **105** (2022) 092002, arXiv:2202.07288 [hep-ex].
31. ATLAS Collaboration, *Combination of Searches for Resonant Higgs Boson Pair Production Using pp Collisions at $\sqrt{s} = 13$ TeV with the ATLAS Detector*, Phys. Rev. Lett. **132** (2024) 231801, arXiv:2311.15956 [hep-ex].